Chapter 8

Estimation of potential evapotranspiration using INSAT-3D satellite data over an agriculture area

Prachi Singh[1], **Prashant K. Srivastava**[1,2], **R.K. Mall**[2]

[1]*Remote Sensing Laboratory, Institute of Environment and Sustainable Development, Banaras Hindu University, Varanasi, Uttar Pradesh, India;* [2]*DST-Mahamana Centre of Excellence in Climate Change Research, Institute of Environment and Sustainable Development, Banaras Hindu University, Varanasi, Uttar Pradesh, India*

1. Introduction

Evapotranspiration is considered as one of the most important components of the hydrological cycle. On the Earth's surface, evapotranspiration plays an important role in context of water-energy balance and irrigation, as well as agriculture practices. The watershed hydrology is influenced by the global climate change as a result of varying evapotranspiration (ET) processes at different scales (Rao et al., 2011; Srivastava et al., 2013). Evapotranspiration (ET) is the combined loss of water in the form of evaporation from the soil surface and transpiration from the plant through the stomata (Kar et al., 2016). There are several methods available to estimate ET, but the most robust method is the Hamon's method, which needs minimal amount of data to calculate this variable. Hydro-meteorological applications such as assessment of climate and analysis of human-induced effects on natural and agricultural ecosystem require various parameters at local as well as regional scales (Rao et al., 2011; Srivastava et al., 2016).

Evapotranspiration (ET) is one of the most useful hydrological fluxes used for maintaining water balance of the terrestrial ecosystems. Reliable and accurate quantification of changes in ET is imperative for effective irrigation management, crop yield forecast, environmental assessment, ecosystem modelling and solar energy system (Almorox and Hontoria, 2004; Khoob, 2008; Singh and Pawar, 2011; Amatya et al., 2014; Petropoulos et al., 2018). For assessment of ET some conventional methods have been used such as

Agricultural Water Management. https://doi.org/10.1016/B978-0-12-812362-1.00008-4

weighing lysimeter, Energy Balance Bowen Ratio (EBBR), eddy covariance techniques, pan-measurement, sap flow, and scintillometer. They are mainly based on a variety of complex models and are limited to local, field and landscape scales (Liou and Kar, 2014). Potential evapotranspiration (PET) is mainly used to measure the actual evapotranspiration that is difficult to assess using these conventional methods (Liou and Kar, 2014). Assessment of accurate PET is useful for many applications including irrigation scheduling, drought monitoring and understanding climate change impacts (Allen et al., 2007; Senay et al., 2007; Wagle et al., 2017; Petropoulos et al., 2015).

However assessing or modelling PET is the most difficult task especially at global scales. Reason is that the traditional approaches can accurately measure ET over homogeneous areas but cannot be directly extended to large-scale ET, due to natural heterogeneity of the land surface and complexity of hydrologic processes and because of the need for a variety of surface measurements and land surface parameters (Thakur et al., 2011; Srivastava et al., 2017). In this context, remote sensing proves to be a cost-effective approach to assess PET at both regional and global scales. Satellite-derived remote sensing images are a promising source, which provides data for mapping regional- and meso-scale patterns of PET on the Earth's surface and surface temperature helps to establish the direct link between surface radiances and energy balance components (Bartholic and Wiegand, 1970; Idso et al., 1975a; Idso et al., 1975b,c; Jackson, 1985; Caselles et al, 1992; Kustas and Norman, 1996). Information can be obtained from different regions of EMR viz. visible, near-infrared, and thermal infrared regions which can be utilized to determine the land surface temperature (LST) and atmospheric temperature. These important surface and atmospheric parameters then serve as inputs to simulate surface fluxes and PET based on the energy balance equation (Srivastava et al., 2020). Remote sensing tool extends a large and continuous spatial coverage within a short period. It is a cost-effective way of measuring ET compared to the conventional measurements, and it is the only approach for ungauged areas where manual measurements are extremely difficult to conduct (Rango, 1994; Schultz and Engman, 2012). Spatially retrieved surface temperature can provide a surface measurement from a resolution of a few cm^2 to several km^2 from certain satellites (Hatfield, 1983). Remote sensing−based ET estimation and its development have been reviewed from time to time (Moran and Jackson, 1991; Kustas and Norman, 1996' Quattrochi and Luvall, 1999).

Bastiaanssen developed SEBAL model for estimation of ET and used satellite remote sensing techniques for knowledge of spatiotemporal distribution of ET on large scale, and it can provide important information on issues related such as evaluating water distributions, water use by different land surfaces, water allocations, water rights, consumptive water use and planning, and also better management of ground and surface water resources

(Singh et al., 2008). As we know for the study of water rights management and water regulation and also for the quantification of ET irrigated projects have been playing a main role. Traditionally, ET has been calculated by using weather-based reference ET by crop coefficients (K_c) that depend upon the crop type and the crop growth stage (Allen et al., 2005). This study provided the estimation of evapotranspiration using temperature data of INSAT-3D over an agricultural area of Northern India.

2. Materials and methodology

2.1 Study area

In this study, Varanasi district of Uttar Pradesh was used as a study area, which lies geographically between 25°14′ 54.94″ N to 25.17′ 06.57″ N and 82° 58′ 30″ E to 83° 00′ 35″E and mean elevation of 80.71 m from the Mean Sea Level (MSL) (Cai et al., 2009). This study area mainly consists of agriculture landscape and is also part of Indo-Gangetic plain that supports good agricultural productivity, and the land is composed of very fertile alluvial soil deposited by the River Ganga and Varuna. Varanasi lies in the humid subtropical climatic zone that is characterized by the hot summer having a temperature between 22 to 46°C and winters with a temperature drop of up to 5°C. The mean annual rainfall is about 1056 mm (+172 SD) (Mall and Gupta, 2002). According to the study of Rao et al. (1971) Potential ET estimated approximately 1525 mm/year. The percentage distribution of annual rainfall for Varanasi district was recorded season-wise. Firstly, for monsoon season (June to September) it was about 88%; likewise, for winter season 7.7% (October to February) and lastly for summer season (March to May) 4.3%. whereas, about 90% of the total rainfall takes place in monsoon season from June to September. Lowest temperature recorded in the last week of December and first week of January is about 9.3°C, and highest temperature reaches maximum by the end of May or early June. During winter season normally wheat crops are planted and harvested in April to May month. The soil of the study area is alluvial in origin. Ustochrepts and Ustifluvents groups define the six categories of soil for Varanasi district. Those groups belong to USDA soil taxonomy (Singh et al., 1989). Soil texture found for this study area is 15%−30% clay and 30%−70% sand. The profile is 1.2 m deep (Mall and Gupta). In this study, data was collected from department of Agriculture Farm of Institute of Agricultural Sciences, B.H.U., Varanasi. Gravimetric lysimeter (mechanical weighing) instrument was used for daily ET data collection. India Meteorological Department installed this instrument which comes in fully fabricated design. Lysimetric data are available for long periods, especially for crop season. For the estimation of ET data weather data temperature were collected from the study site.

2.2 INSAT-3D

INSAT series of multipurpose spacecrafts have been providing meteorological services over Indian Ocean since early eighties through Very High Resolution Radiometer instruments. Kalpana-1 launched in 2002 was the first dedicated met satellite of ISRO. ISRO plans to deploy a new generation dedicated met satellite INSAT-3D over Indian Ocean in 2007−2008 time frame. This chapter presents an overview of the INSAT 3D mission and a detailed description of its Met Payloads, viz., Imager and Sounder (Rani and Prasad, 2013).

Indian National Satellite System (INSAT) is a set of geostationary satellites launched by ISRO in which INSAT-3D is an advanced geostationary meteorological satellite launched on 26 July 2013 from French Guiana using ARIANE rocket (Hawkins et al., 2008). The major applications of INSAT-3D are to improve imaging system for meteorological observations, land surface monitoring and vertical profile generation for weather forecasting and disaster predictions. It is one of the famous satellites developed by ISRO to enhance domestic weather forecasting and also useful for tracking cyclones and monsoons originating from Bay of Bengal and Arabian Sea. INSAT-3D is located at 82° east. It carries a multispectral imager (optical radiometer) for meteorological operations and produces images of Earth in six wavelength bands (Mishra et al., 2014).

This instrument has meteorological payloads on board the spacecraft:

- Six-channel imaging radiometer intended to estimate radiant and solar reflected energy from Earth.
- Nineteen-channel sounder for measuring vertical temperature profiles, humidity as well as for ozone distribution.
- Data relay transponder (DRT) useful to provide data collection and data dissemination using data collection platforms
- Satellite-aided search and rescue (S&SR) system (Katti et al., 2006).

Present study is based on the LST product of INSAT-3D Imager which provides data per day with a temporal resolution of $0.5° \times 0.5°$ which can be downloaded from MOSDAC website (https://mosdac.gov.in/data/).

2.2.1 Instrument detail

2.2.1.1 Imager

INSAT-3D has four meteorological payloads that are mainly designed to observe solar and radiant energy for sampled areas of the Earth's surface. Imager payloads have six imaging radiometer channels, in which one is visible, and five are infrared channels. These channels are designed to observe radiant and solar reflected energy (Pandya et al., 2011). INSAT-3D

Imager can be considered an enhanced version of Very High Resolution Radiometer (VHRR), Series of INSAT five original instruments flown on INSAT 2A through INSAT 3A satellites and on Kalpana-1.

INSAT-3D Imager spectral channels are very comparable to those of five channel of NOAA GOES Imager but diverse for additional channels in the Short Wave IR (SWIR) band. INSAT-3D generates Earth image in six spectral channels and for scanning the Earth's disk it uses scan mirror ascended on two axes Gimbal. The Visible and SWIR channels hold ground resolution at nadir 1 and 8 km in water vapour band. Sufficient radiometric resolution and dynamic range are provided for all channels to understand the application science goals. INSAT-3D is also capable of generating full Earth disk image in 26 min. A flexible scan pattern allows tradeoff between the coverage and the imaging periodicity. Visible band is useful for the monitoring of mesoscale phenomena and severe local storms. And the other two new bands, SWIR with resolution of 1 km and MWIR 4 km, will enable improved land-cloud discrimination and detection of surface features like snow. INAST-3D has TIR channel that holds 4 km resolution with two separate windows in 10.2−11.2 and 11.5−12.5 μm regions. INSAT-3D has some modules, one of which is the EO (electro-optics) module which containing the telescope, scan assembly and detectors with cooler facility. This module is mounted on the external part of spacecraft, and in the internal part of the spacecraft all electronic packages are installed. It has a total mass of ∼130 kg (Misra and Kirankumar 2014).

2.2.1.2 Sounder

INSAT-3D sounder is the first geostationary INSAT series instrument being developed by ISRO. The main objective of this instrument is to measure temperature and humidity profiles that are also known as vertical distributions. Vertical profiles of temperature and humidity are mainly enabled by sounder. These vertical profiles can then be used to obtain various atmospheric stability indices and other parameters such as atmospheric water vapour content and total column ozone amount. It can obtain three-dimensional representation of the atmosphere. Sounder has 19 spectral channels which are used to measure radiation; it is useful to sense specific data parameters for atmospheric vertical temperature and moisture profiles, surface and cloud top temperature and ozone distribution. Eighteen narrow channels are distributed over three IR bands (seven long-wave (LW), five mid-wave (MW), six short-wave (SW)), while one is a broad visible channel (Katti et al., 2006). Sounder uses two axes gimbaled scan mirror for measuring radiance in 18 IR and one visible channel oven an area of 10*40 km at nadir every 100 ms. INSAT 3D Sounder is very similar to the NOAA GOES Sounder instruments. Sounder provides acceptable radiometric

resolution that is useful for application of science. The operation of the Sounder is limited by ground commands using some parameters like gain, sounding area location and other such parameters, and sounding area is defined in terms of east−west and north−south 'blocks'. Like imager payload, sounder also has EO (electro-optics) module as well as collection of electronic packages with power supply modules. These modules hold telescope, scan assembly, filter wheels and coolers and work like imager instrument mounted in the internal part of spacecraft. It contains a total mass of ∼145 kg (Prasad et al., 2009).

2.2.1.3 DRT (Data Relay Transponder)

Data Relay Transponder is a meteorological payload of INSAT-3D satellite; its main focus is to receive global meteorological, hydrological and oceanographic data from automatic DCPs (Data Collection Platforms). That data stores in the ground segment and relays back to downlink in extensive C-band. The satellites which have enabled DCPs can provide easily a great solution for gathering large amount of meteorological data from all over the country including inaccessible and remote areas. In the collaboration of IMD (Indian Meteorological Department) and ISRO more than 1800 DCPs have been established that will be more helpful for meteorological data collection (Bhattacharya et al., 2009).

2.2.1.4 SAS&R (Satellite Aided Search & Rescue)

SAS&R (Satellite Aided Search & Rescue) is meteorological payload that mainly focuses on relaying a distress signal/alert detection from the beacon transmitters for search and rescue purposes with global receive coverage in UHF band and it operates at 406 MHz (Rani et al., 2016). The downlink operates in extended C-band. The data are transmitted to INMCC (Indian Mission Control Center), located at ISTRAC (ISRO Telemetry, Tracking and Command Network), Bangalore (Prabhu, 2017).

2.3 Hamon's method

In this study, Hamon's method is used as a standard method for calculation of PET. As we know, it is very difficult to get large number of data like solar radiation, wind speed, rainfall. So, to overcome this problem Hamon's method was used in this study that used only minimal amount of data. Hamon's method used only temperature data for estimation of PET. Because of using minimal amount of data Hamon's method is a very simple and robust method for calculating ET (McCabe et al., 2015). PET is calculated using INSAT-3D satellite data, as well as compared with the observed PET Eq. (8.1).

Hamon's equation can be expressed as follows:

$$PET = K * 0.165 * 216.7 * n * \left(\frac{e_s}{T + 273.3}\right) \tag{8.1}$$

where PET is in (mm/day); k is the proportionality coefficient; N is the daytime length; e_s is the saturation vapour pressure (mb) and T is the average monthly temperature. Saturation vapour pressure (e_s) can be calculated using Eq. (8.2).

$$e_s = 6.108_e \left(\frac{17.27T}{T + 273.3}\right) \tag{8.2}$$

3. Performance analysis

In this study PET was assessed from land surface temperature data of INSAT-3D satellite and compared with the observed dataset. For understanding the performance analysis between datasets some statistics used correlation coefficient (r), absolute bias and RMSE (root mean square error). Correlation coefficient measured association between two variables that variables indicate the strength and suitable direction of their relationship (Matrix and Variable).

The correlation coefficient (r) is calculated using this Eq. (8.3).

$$r = \frac{n\sum xy - (\sum x)(\sum y)}{\sqrt{\left[n\sum x^2 - (\sum x)^2\right]\left[n\sum y^2 - (\sum y^2)\right]}} \tag{8.3}$$

To measure model performance in meteorology, air quality and climate research, studies root mean square error (RMSE) has been used as a standard statistical metric (Chai and Draxler, 2014).

RMSE (Root Mean Square Error) is calculated using this Eq. (8.4):

$$RMSE = \sqrt{\left(\frac{1}{n}\sum_{i=1}^{n}[y_i - x_i]^2\right)} \tag{8.4}$$

Bias used to understand under- or overestimate of the true value. Absolute bias is mainly useful to remove faulty measuring devices or procedures and also absolute bias calculates to understand the positive or negative deviation from the actual and observed value (Koch et al., 1982; Walther and Moore, 2005).

Bias is calculated using this Eq. (8.5):

$$\boldsymbol{Bias} = (\overline{\boldsymbol{y}} - \overline{\boldsymbol{x}}) \tag{8.5}$$

where x and y are observed and estimated values respectively. $\overline{\boldsymbol{x}}$ and $\overline{\boldsymbol{y}}$ are the mean of observed and estimated measurements, respectively and n is the total no. of observations.

4. Results and discussions

4.1 Evaluation of temperature data from INSAT-3D and ground base

In this study, land surface temperature was extracted from satellite data and observed datasets. Comparison of temperature derived from INSAT-3D and observed data is showing gradual variations that can be shown in (Fig. 8.1). In line graph, it can be clearly seen that both the temperatures are showing very close relation with each other. Performance statistics are shown in (Fig. 8.2). Correlation (r = 0.733), Bias (−2.030) and RMSE (4.993) was

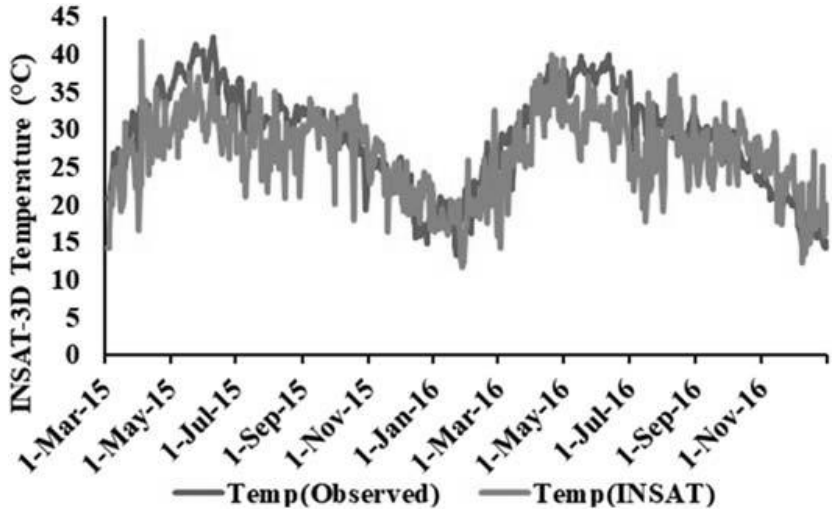

FIGURE 8.1 INSAT-3D daily temperature with observed datasets.

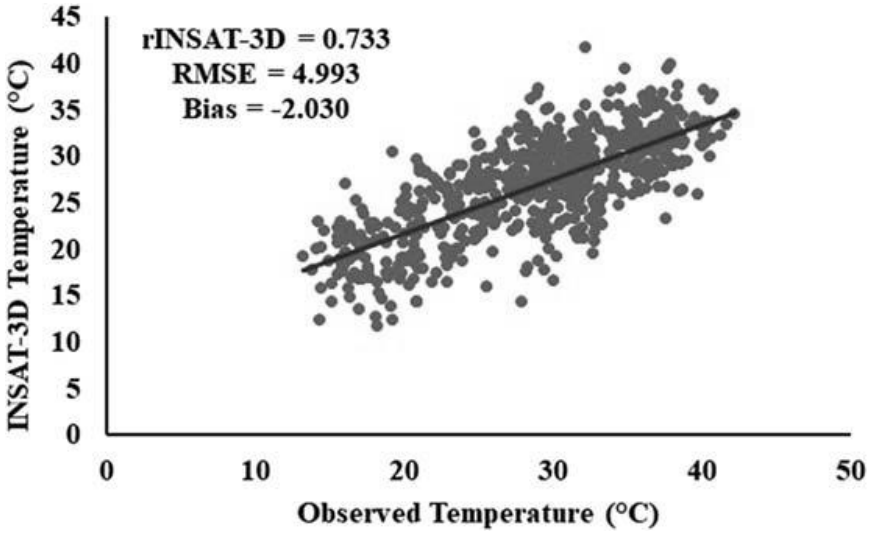

FIGURE 8.2 Scatter plot representing INSAT-3D daily temperature with observed datasets.

observed when INSAT-3D data was compared with that of observed temperature data indicating a close agreement of temperature with in-situ observation. A higher temperature was recorded in summer months (April to June), with gradual increase in both the temperature datasets. In terms of RMSE and bias, INSAT-3D showed a satisfactory performance with observed temperatures datasets (Fig. 8.2).

4.2 Comparative assessment of evapotranspiration products

PET calculated using land surface temperature of INSAT-3D satellite data over agricultural area in Northern India was compared with the observed dataset. The relative plot of INSAT-3D data with observed PET is shown in Fig. 8.3. The PET increases during the months of summer season and decreases in winter season. INSAT-3D data showed an underestimation most of the time (Fig. 8.4). Higher PET was observed from April to July months; this may be due to the very high temperatures in these months. Correlation (r) = 0.572, Bias = 0.524 and RMSE = 0.834 are found between PET of INSAT-3D and observed data. Overall, INSAT-3D data showed highest discrepancies (Fig. 8.4). PET estimation has been done on an annual basis using Hamon's method and values are compared with the annual observed PET. It is clear that PET estimated using INSAT-3D is in marginal agreement with observed PET in annual datasets. The INSAT-3D PET values were always found to be higher

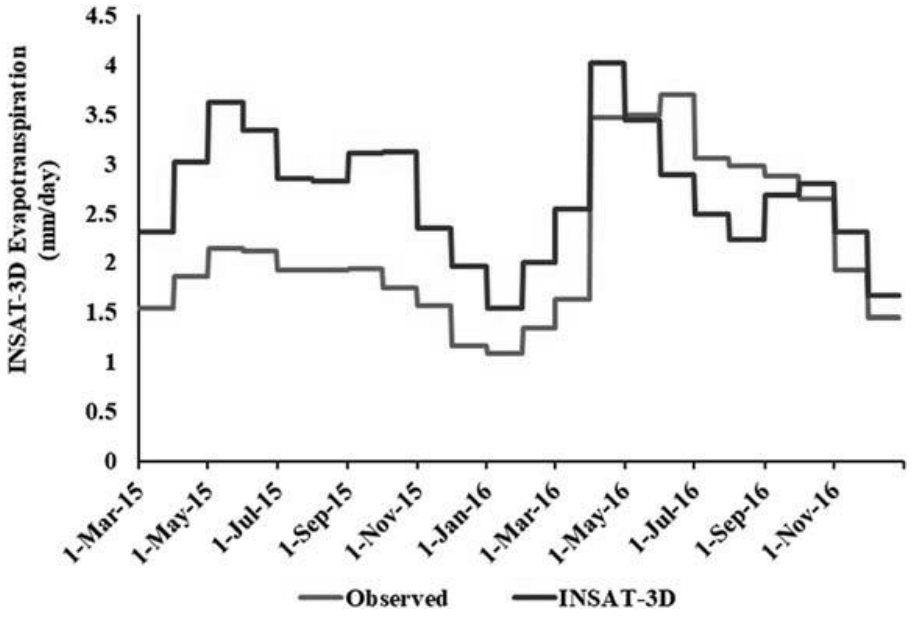

FIGURE 8.3 INSAT-3D daily PET with observed datasets.

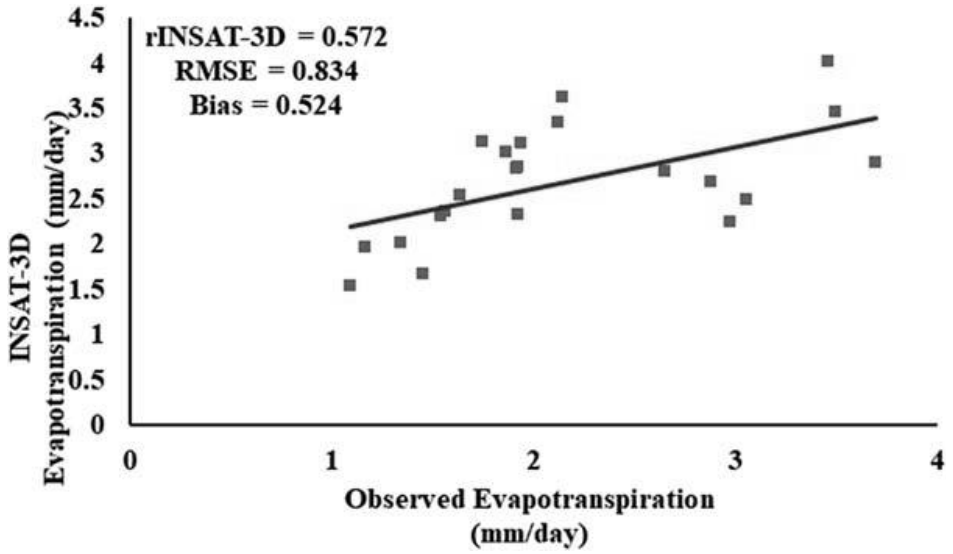

FIGURE 8.4 Scatter plot representing INSAT-3D daily PET with observed datasets.

in comparison to observed PET values. It is clearly seen in Fig. 8.4. Bias and RMSE values were higher when compared with the observed dataset. so, it indicates INSAT-3D dataset could be promising, but needs more research regarding the quality. Further, as Hamon's method has some limitations, better models like Penman Monteith may improve the estimation of PET.

5. Conclusions

In hydrological modelling, weather research and prediction of flood and drought and accurate estimation of potential evapotranspiration could be very helpful. Evapotranspiration plays a very important role in hydrological modelling. Land surface temperature data of INSAT-3D satellite is used for calculation of potential evapotranspiration (PET). This study has brought out useful information about evapotranspiration in Varanasi district. The PET values are calculated using the Hamon's method. Hamon's method does not depend upon any other factor; only climatic factors are enough for this estimation. The PET values estimated from the INSAT-3D showed some overestimation as compared to observed PET values from station datasets. Comparison of INSAT-3D evapotranspiration shows a promising match with the observed dataset in terms of trend. The comparison of PET showed quite a close correlation. This study can improve forecasting application and effectiveness of hydro-meteorological modelling. Accurate information of evapotranspiration can provide incredible support in the study of sustainable water resource management (Srivastava et al., 2016). However, the study has lot of potential and could be extended over other regions where relevant data are available.

References

Allen, R.G., Tasumi, M., Morse, A., Trezza, R., 2005. A Landsat-based energy balance and evapotranspiration model in Western US water rights regulation and planning. Irrigat. Drain. Syst. 19 (3), 251–268.

Allen, R.G., Tasumi, M., Trezza, R., 2007. Satellite-based energy balance for mapping evapotranspiration with internalized calibration (METRIC)—model. J. Irrigat. Drain. Eng. 133 (4), 380–394.

Almorox, J., Hontoria, C., 2004. Global solar radiation estimation using sunshine duration in Spain. Energy Convers. Manag. 45 (9–10), 1529–1535.

Amatya, D.M., Harrison, C.A., Trettin, C.C., 2014. Comparison of Potential Evapotranspiration (PET) Using Three Methods for a Grass Reference and a Natural Forest in Coastal Plain of South Carolina.

Bartholic, J., Wiegand, C., 1970. Remote Sensing in Evapotranspiration Research on the Great Plains.

Bhattacharya, B., Mallick, K., Padmanabhan, N., Patel, N., Parihar, J., 2009. Retrieval of land surface albedo and temperature using data from the Indian geostationary satellite: a case study for the winter months. Int. J. Remote Sens. 30 (12), 3239–3257.

Cai, X., Wang, D., Laurent, R., 2009. Impact of climate change on crop yield: a case study of rainfed corn in central illinois. J. Appl. Meteorol. & Climatol. 48 (9), 1868–1881.

Caselles, V., Sobrino, J., Coll, C., 1992. On the use of satellite thermal data for determining evapotranspiration in partially vegetated areas. Int. J. Remote Sens. 13 (14), 2669–2682.

Chai, T., Draxler, R.R., 2014. Root mean square error (RMSE) or mean absolute error (MAE)? –arguments against avoiding RMSE in the literature. Geosci. Model Dev. (GMD) 7 (3), 1247–1250.

Cheruku, D.R., 2010. Satellite Communication. IK International Pvt Ltd.

Hatfield, J., 1983. Evapotranspiration obtained from remote sensing methods. Adv. Irrig. 2, 395–416. Elsevier.

Hawkins, G., Sherwood, R., Barrett, B., Wallace, M., Orr, H., Matthews, K., Bisht, S., 2008. High-performance infrared narrow-bandpass filters for the Indian National Satellite System meteorological instrument (INSAT-3D). Appl. Optic. 47 (13), 2346–2356.

Idso, S., Schmugge, T., Jackson, R., Reginato, R., 1975a. The utility of surface temperature measurements for the remote sensing of surface soil water status. J. Geophys. Res. 80 (21), 3044–3049.

Idso, S.B., Jackson, R.D., Reginato, R.J., 1975b. Detection of soil moisture by remote surveillance: difficult problems limit immediate applications, but the potential social benefits call for serious attempts at their solution. Am. Sci. 63 (5), 549–557.

Idso, S.B., Jackson, R.D., Reginato, R.J., 1975c. Estimating evaporation: a technique adaptable to remote sensing. Science 189 (4207), 991–992.

Jackson, R.D., 1985. Evaluating evapotranspiration at local and regional scales. Proc. IEEE 73 (6), 1086–1096.

Kar, S.K., Nema, A., Singh, A., Sinha, B., Mishra, C., 2016. Comparative study of reference evapotranspiration estimation methods including Artificial Neural Network for dry sub-humid agro-ecological region. J. Soil Water Conserv. 15 (3), 233–241.

Katti, V., Pratap, V., Dave, R., Mankad, K., 2006. INSAT-3D: An Advanced Meteorological Mission over Indian Ocean. GEOSS and Next-Generation Sensors and Missions. International Society for Optics and Photonics.

Khoob, A.R., 2008. Comparative study of Hargreaves's and artificial neural network's methodologies in estimating reference evapotranspiration in a semiarid environment. Irrigat. Sci. 26 (3), 253–259.

Koch, G.G., Kotz, S., Johnson, N., Read, C., 1982. Encyclopedia of Statistical Sciences, vol. 213. J Wiley, New York, p. 7.

Kustas, W., Norman, J., 1996. Use of remote sensing for evapotranspiration monitoring over land surfaces. Hydrol. Sci. J. 41 (4), 495–516.

Liou, Y.-A., Kar, S.K., 2014. Evapotranspiration estimation with remote sensing and various surface energy balance algorithms—a review. Energies 7 (5), 2821–2849.

Mall, R., Gupta, B., n.d. Comparison of Evapotranspiration Models.

Mall, R., Gupta, B., 2002. Comparison of evapotranspiration models. Mausam 53 (2), 119–126.

Matrix, C., Variable, I. n.d.Correlation Coefficient (r).

McCabe, G.J., Hay, L.E., Bock, A., Markstrom, S.L., Atkinson, R.D., 2015. Inter-annual and spatial variability of Hamon potential evapotranspiration model coefficients. J. Hydrol. 521, 389–394.

Mishra, M.K., Rastogi, G., Chauhan, P., 2014. Operational retrieval of aerosol optical depth over Indian subcontinent and Indian ocean using INSAT-3D/imager and product validation. ISPRS–Int. Arch. Photogramm. Remote Sens. & Spat. Inf. Sci. 8, 277–282.

Misra, T., Kirankumar, A., 2014. A glimpse of ISRO's EO programme [Space Agencies]. IEEE Geosci. & Remote Sens. Mag. 2 (4), 46–53.

Moran, M.S., Jackson, R.D., 1991. Assessing the spatial distribution of evapotranspiration using remotely sensed inputs. J. Environ. Qual. 20 (4), 725–737.

Navalgund, R.R., Jayaraman, V., Roy, P., 2007. Remote sensing applications: an overview. Curr. Sci. 93 (12), 00113891.

Pandya, M., Shah, D., Trivedi, H., Panigrahy, S., 2011. Simulation of at-sensor radiance over land for proposed thermal channels of imager payload onboard INSAT-3D satellite using MODTRAN model. J. Earth Syst. Sci. 120 (1), 19–25.

Petropoulos, G.P., Ireland, G., Cass, A., Srivastava, P.K., 2015. Performance assessment of the SEVIRI evapotranspiration operational product: results over diverse mediterranean ecosystems. IEEE Sens. J. 15 (6), 3412–3423.

Petropoulos, G.P., Srivastava, P.K., Piles, M., Pearson, S., 2018. Earth observation-based operational estimation of soil moisture and evapotranspiration for agricultural crops in support of sustainable water management. Sustainability 10 (1), 181.

Prabhu, B., 2017. A Research on Sensors and Positioning of INSAT-3D.

Prasad, M., Akkimaradi, B., Selvan, T., Rastogi, S., Badrinarayana, K., Bhandari, D., Sugumar, M., Mallesh, B., Rajam, K., Rajgopalan, I., 2009. Development of Sunshield Panels for Passive Radiant Cooler on Board Meteorological Instruments of ISRO.

Quattrochi, D.A., Luvall, J.C., 1999. Thermal infrared remote sensing for analysis of landscape ecological processes: methods and applications. Landsc. Ecol. 14 (6), 577–598.

Rango, A., 1994. Application of remote sensing methods to hydrology and water resources. Hydrol. Sci. J. 39 (4), 309–320.

Rani, S.I., Prasad, V., 2013. Simulation and Validation of INSAT-3D Sounder Data at NCMRWF.

Rani, S.I., Prasad, V., Rajagopal, E., Basu, S., 2016. Height of warm core in very severe cyclonic storms Phailin: INSAT-3D perspective. In: Remote Sensing and Modeling of the Atmosphere, Oceans, and Interactions VI. International Society for Optics and Photonics.

Rao, K., George, C., Ramasastri, K., 1971. Potential evapotranspiration over India. India Met. Dept. Sci. Rep 136.

Rao, L., Sun, G., Ford, C., Vose, J., 2011. Modeling potential evapotranspiration of two forested watersheds in the southern Appalachians. Trans. ASABE 54 (6), 2067–2078.

Schultz, G.A., Engman, E.T., 2012. Remote Sensing in Hydrology and Water Management. Springer Science & Business Media.

Senay, G.B., Budde, M., Verdin, J.P., Melesse, A.M., 2007. A coupled remote sensing and simplified surface energy balance approach to estimate actual evapotranspiration from irrigated fields. Sensors 7 (6), 979–1000.

Singh, G., Agrawal, H., Singh, M., 1989. Genesis and classification of soils in an alluvial pedogenic complex. J. Indian Soc. Soil Sci. 37 (2), 343–354.

Singh, R.K., Irmak, A., Irmak, S., Martin, D.L., 2008. Application of SEBAL model for mapping evapotranspiration and estimating surface energy fluxes in south-central Nebraska. J. Irrigat. Drain. Eng. 134 (3), 273–285.

Singh, R.K., Pawar, P., 2011. Comparative study of reference crop evapotranspiration (ETo) by different energy based method with FAO 56 Penman-Monteith method at New Delhi, India. Int. J. Eng. Sci. Technol. 7861–7868.

Srivastava, P.K., Han, D., Islam, T., Petropoulos, G.P., Gupta, M., Dai, Q., 2016. Seasonal evaluation of evapotranspiration fluxes from MODIS satellite and mesoscale model downscaled global reanalysis datasets. Theor. Appl. Climatol. 124 (1–2), 461–473.

Srivastava, P.K., Han, D., Rico Ramirez, M.A., Islam, T., 2013. Comparative assessment of evapotranspiration derived from NCEP and ECMWF global datasets through Weather Research and Forecasting model. Atmos. Sci. Lett. 14 (2), 118–125.

Srivastava, P.K., Han, D., Yaduvanshi, A., Petropoulos, G.P., Singh, S.K., Mall, R.K., Prasad, R., 2017. Reference evapotranspiration retrievals from a mesoscale model based weather variables for soil moisture deficit estimation. Sustainability 9 (11), 1971.

Srivastava, P.K., Singh, P., Mall, R., Pradhan, R.K., Bray, M., Gupta, A., 2020. Performance assessment of evapotranspiration estimated from different data sources over agricultural landscape in Northern India. Theor. Appl. Climatol. 140 (1–2), 145–156.

Thakur, J.K., Srivastava, P., Pratihast, A.K., Singh, S.K., 2011. Estimation of evapotranspiration from wetlands using geospatial and hydrometeorological data. In: Geospatial Techniques for Managing Environmental Resources. Springer, Netherlands, pp. 53–67. Springer.

Wagle, P., Bhattarai, N., Gowda, P.H., Kakani, V.G., 2017. Performance of five surface energy balance models for estimating daily evapotranspiration in high biomass sorghum. ISPRS J. Photogramm. Remote Sens. 128, 192–203.

Walther, B.A., Moore, J.L., 2005. The concepts of bias, precision and accuracy, and their use in testing the performance of species richness estimators, with a literature review of estimator performance. Ecography 28 (6), 815–829.